Frequency-Dependent Impedance Responses of ZnO Using UV Light

Jiaqi Cheng[1] **and Kristin M. Poduska**[1,2,*,z]

[1]*Department of Chemistry, Memorial University of Newfoundland, St. John's, NL A1B 3X7, Canada*
[2]*Department of Physics and Physical Oceanography, Memorial University of Newfoundland, St. John's, NL A1B 3X7, Canada*

Impedance spectroscopy data show that polycrystalline ZnO films can show either increases or decreases in their effective resistances after UV exposure, depending on the frequency of the applied AC excitation. Simple equivalent circuit models, based on resistance (R) and capacitance (C) in parallel, are sufficient to confirm the observed experimental trends. Simulated data demonstrate that that arbitrary R and C values will not produce the sign change, but that typical resistance and capacitance characteristics for photoconductive semiconductors like ZnO can cause the sign change. These results suggest that it could be desirable to manipulate the R and C values of photodetector materials to either control – or eliminate – such frequency-dependent UV responses.
 [DOI: 10.1149/2.0041901jss]

Manuscript submitted August 27, 2018; revised manuscript received December 31, 2018. Published January 10, 2019.

The conductivity changes that occur in some materials upon exposure to UV light has sparked a wide range of applications in optoelectronics,[1] flame sensing,[2] and biosensing.[3] Among the many wide-bandgap semiconductors that have been explored for UV sensors,[2] ZnO has attracted extensive attention because of its relatively low cost, ease of production, and rich surface chemistry.[1,3]

The mechanism behind electrical resistance changes upon exposure to light can vary among different materials.[2] For ZnO, studies have shown that surface states play a dominant role in photoconductivity.[4,5] When light shines on ZnO, it absorbs photons that generate electron-hole pairs in the bulk. These photo-generated holes migrate to the surface and neutralize adsorbed oxygen ions (O_2^-) that form readily forms ZnO surfaces under ambient conditions. This causes O_2 desorption; the photo-generated electron that remains in the ZnO causes a conductivity increase. Thus, based on this mechanism, the photoresponse of ZnO is controlled by the O_2 adsorption/desorption equilibrium at surfaces. This has led to a flourish of research activity related to ZnO powders, wires, and rods because their large surface-volume ratios tend to cause a stronger photoconductive response.[2,6,7]

Photoconductivity of polycrystalline ZnO films and nanostructures have been explored not only with direct current (DC) excitations, but also as a function of alternating current (AC) excitations using impedance spectroscopy. AC-dependent conductivity trends are particularly important for assessing how the ZnO would function in a capacitance-based sensor, since the time required for capacitor charging and discharging could influence sensor response times. Impedance spectra of nanocrystalline ZnO films taken before and during UV exposure, showed that small average grain sizes, high porosity, and specific kinds of surface chemistries increase DC and AC conductivity.[8] More recently, electrochemical impedance spectroscopy was paired with gas chromatography mass spectrometry (GC-MS) to probe the chemical origin of the UV responses of ZnO nano-crystalline film in an ambient environment.[5] That work showed that ZnO impedance changes are correlated with desorption of O_2, water and other organic byproducts from ZnO surfaces *via* UV induced photochemistry.

In this study, we show an interesting and surprising effect: depending on the AC excitation frequency, UV light can cause either an increase or a decrease in its apparent resistance. We demonstrate that this behavior is consistent with UV-induced changes in film's resistance, based on simulated data based on equivalent circuit modeling. Based on the simplicity of the origin effect, we proposed that it could be generalizable to other photoconductive materials.

*Electrochemical Society Member.
[z]E-mail: kris@mun.ca

Experimental

ZnO film preparation.—ZnO powder was synthesized using a room-temperature solid-state metathesis reaction that is described in an earlier publication.[9] The starting materials, $ZnCl_2$ and NaOH, were ground into fine powders using an agate mortar and pestle. They were then mixed together (1:2 molar ratio) in a glass beaker, during which an exothermic reaction produced a white paste. Filtering with ultrapure water (Barnstead Nanopure, 18.2 MΩ·cm) removed the NaCl by-product, leaving the desired ZnO solid. After air drying for several hours, the powder was heated for 8 hours at 500°C, ramping and cooling at a rate of 100°C per hour. A ZnO slurry was then prepared from 0.10 g of the annealed powder that was dispersed in 2 mL of 1:1 ethanol/water mixture. After 30 s of ultrasonication, the slurry was spread by hand over an electrically conductive indium tin oxide (ITO) coated glass slide (8-12 Ω, Delta Technology). A second ITO electrode was pressed on top, held in place by binder clips, to sandwich the ZnO film.

Photoresponse measurements.—Prior to the measurements, ZnO films were allowed to equilibrate for 24 h in a dark box under steady humidity levels that were controlled using saturated salt solutions.[10,11] All measurements were conducted at room temperature (22 ± 2°C). The UV lamp (365 nm emission, Model UVGL-25, UVP Inc.) had an intensity of 1.6 mW cm^{-2} at a distance of 5 cm.

Impedance spectroscopy was performed using a Princeton Applied Research potentiostat/galvanostat (Model 273A with Signal Recovery Model 5210 Lock-in Amplifier, input impedance 10 GΩ, Power SUITE software). A sinusoidal AC potential (10 mV RMS amplitude, 0 V DC bias) was swept from 10^5 Hz to 10^{-1} Hz. DC film resistances were measured separately with an inductance-capacitance-resistance (LCR) meter (National Instruments) using a DC test current (0.5 μA; meter range 10 MΩ, resolution 10 Ω).

Equivalent circuit fitting of the EIS data was done manually by superimposing simulated spectra (EIS Spectrum Analyser freeware[12]) onto the raw data and iteratively adjusting parameters. All EIS data described in this work could be modeled well with a circuit containing only one resistor and one capacitor in parallel.

Results and Discussion

Electrical characterization.—Figure 1 shows representative examples of DC resistance changes when ZnO films are exposed to intermittent periods of UV exposure. UV illumination triggers an abrupt resistance decrease. Once the light is removed, the sample resistance returns to the original value after hundreds of seconds. Based on data

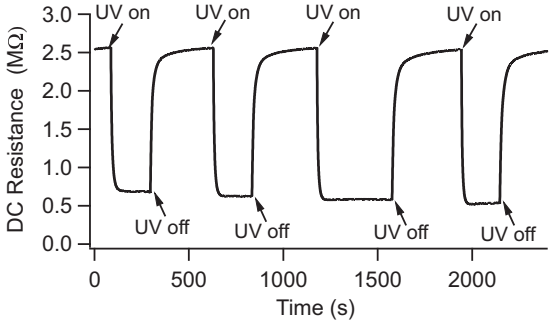

Figure 1. Representative resistance changes for a ZnO film in response to intermittent UV light exposure.

from ten comparably prepared samples, ZnO film resistances were MΩ-range values under dark conditions, and UV exposure reduced the resistance by factors of 2-10.

Fig. 2 compares representative Nyquist and Bode plots for the dark and light impedance behaviors of the ZnO films. Consistent with the DC resistance data, Z_{re} decreases after UV exposure in the low-frequency regime. Z_{im} has a more complicated response as a function of frequency, showing a maximum (labeled f_{max} in Figures 2c,2f). Above this frequency, Z_{re} is no longer frequency independent (labeled f_{max} in Figures 2b,2e).

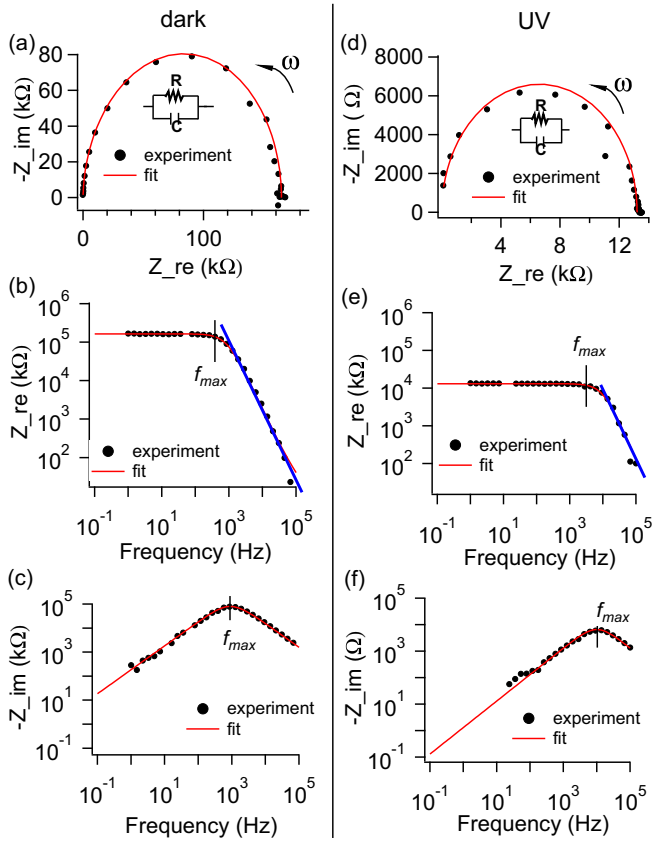

Figure 2. Representative EIS data in the dark (a-c) and under UV illumination (d-f). Experimental data are shown as black dots, and they were fit to an equivalent circuit that is shown in the insets of panels (a) and (d). Arrows in the Nyquist plots (a,d) indicate the direction of increasing frequency (ranging from 0.1 Hz to 100 kHz). Blue fit lines (b,e) highlight the linear portions of the log-log Bode plots for the high frequency range of Z_{re}. f_{max} denotes the maximum frequency before which Z_{re} begins to decrease.

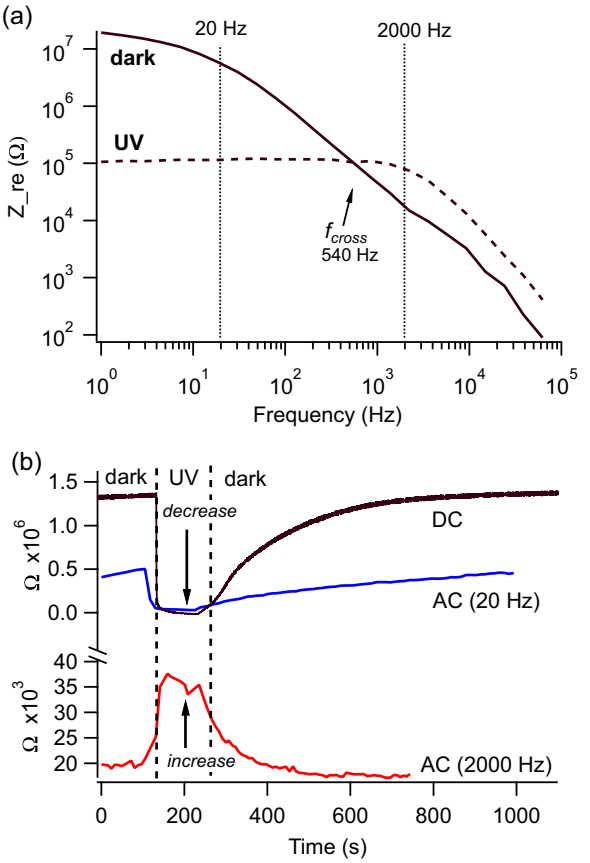

Figure 3. (a) Representative Z_{re} vs. f data taken in the dark and under UV light, with their intersection point ($f_{cross} = 540 \pm 50$ Hz) indicated by an arrow. (b) Representative photoresponses under DC conditions (black), f lower than f_{cross} (20 Hz, shown in blue), and f greater than f_{cross} (2000 Hz, shown in red). The arrows indicate that UV exposure causes an increase in Z_{re} for 2000 Hz excitation, but a decrease for DC or 20 Hz excitation.

An interesting phenomenon appears when one compares the Z_{re} vs. f plots for dark and UV illumination conditions. Figure 3a shows that, when these two Bode plots are overlaid, the spectra intersect at a frequency that we denote as f_{cross}. This crossing suggests that opposite signs for UV-induced resistance changes could occur, depending on the value of the test frequency. Data in Figure 3b confirm this sign change. At frequencies smaller than f_{cross} (either DC or 20 Hz AC), the magnitude of Z_{re} is larger in the dark than in UV. However, for frequencies above f_{cross} (2000 Hz), Z_{re} is larger during UV exposure. Thus, UV exposure can cause either an increase or a decrease in the film resistance, depending on the relation between the excitation frequency and f_{cross}.

Modelling frequency-dependent photoresponses.—We used equivalent circuit modeling to show that f_{cross}, and the associated sign change in the resistive photoresponse, is a robust phenomenon.

Simulated Bode spectra were based on a parallel RC circuit (Figure 4 inset), with varying R and C values (R = 10-1000 kΩ and C = 0.1-100 nF) that included the range we measured for our ZnO films (R = 10-1000 kΩ and C = 0.4-1.4 nF).

The simulations clearly show that changing R and C values result in a shift of Z_{re} spectra. Fig. 4a presents simulation results after decreasing C while keeping R constant. This manipulation leads to a shift of f_{max} toward higher frequencies and does not cause f_{cross}. Fig. 4b shows another scenario: decreasing R while increasing C proportionally, in order to keep the ratio RC constant. In this case, Z_{re} drops over the whole frequency range without intersecting the original spectrum. Fig. 4c shows that f_{cross} occurs when R decreases.

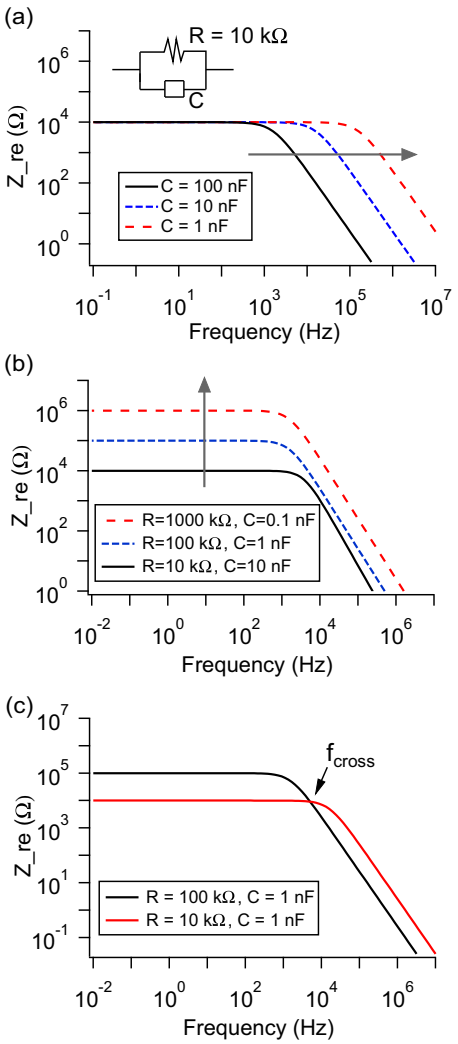

Figure 4. Simulated Z_{re} vs. f data based on a parallel RC circuit shown in (a). In (a), C decreased while R was constant. In (b), R decreased while keeping the ratio RC constant. In (c), f_{cross} occurs when R decreases while C is constant.

Based on these simulations, the occurrence of f_{cross} for a photoresponsive film (based on parallel RC equivalent circuit behavior) must satisfy two conditions. First, $R_{dark} > R_{UV}$. Second, $R_{dark} \times C_{dark} > R_{UV} \times C_{UV}$. These conditions would be easy to satisfy in many ZnO films. A DC resistance decrease during UV exposure is consistent with the ZnO photoresponse mechanism proposed by others.[4,5,13] This means that the first criterion will typically be met in ZnO films. The second criterion would then also be satisfied if UV exposure did not cause a significant capacitance increase.

Relating these simulations to experimental findings, equivalent circuit fits of EIS data show that our ZnO films satisfy the two conditions necessary for f_{cross} to occur. Figure 2 shows that both dark and UV impedance data can be fit well with a simple parallel RC equivalent circuit. Based on R and C values extracted from these fits, UV exposure affects the resistance of the ZnO films much more than the capacitance. For example, the data shown in Figure 2 indicate a resistance change from 150 ± 5 kΩ dark compared to 13.2 ± 0.2 kΩ for UV, while the capacitance shows no appreciable increase (1.0 ± 0.2 nF for dark compared with 1.2 ± 0.2 nF for UV). The fits yielding these R and C values are superimposed over the experimental data in Figure 2.

Equivalent circuit modeling also helps to explain the origin of f_{max} in Figures 2c, 2f. For a parallel RC circuit, the behavior of Z_{im} as a function of frequency follows the relation:

$$Z_{im}(f) = -R\frac{2\pi f\tau}{1+(2\pi f\tau)^2} \quad [1]$$

where τ is the capacitive time constant. This is related to f_{max} by:

$$\tau = RC = \frac{1}{2\pi f_{max}} \quad [2]$$

In log-log form, Eq. 1 can be re-written as:

$$\log[Z_{im}] = \log[f] + \log[-2\pi\tau R] - \log[1+(2\pi f\tau)^2] \quad [3]$$

Written in this form, it is evident that the maximum value of Z_{im} occurs when the applied frequency f matches the inverse of the time constant τ; this is f_{max}. Thus, a peak in the -Z_{im} Bode plot will occur for any system that can be modeled with a parallel RC equivalent circuit.

In a similar way, a parallel RC circuit explains why the real component of the impedance Z_{re} also changes behavior at f_{max}. For an RC equivalent circuit,

$$Z_{re}(f) = \frac{R}{1+(2\pi f\tau)^2} \quad [4]$$

In log-log form:

$$\log[Z_{re}] = \log[R] - \log[1+(2\pi f\tau)^2] \quad [5]$$

For low frequencies ($f \ll f_{max}$), the second term in Equation 5 is negligible, meaning that Z_{re} is related only to the resistance R and is independent of f. However, at high frequencies ($f \gg f_{max}$), $Z_{re} \rightarrow R/(2\pi f)^2$. When plotted on a log-log scale (Figs. 2b, 2e), the manifestation of f_{max} is the frequency at which the roll-off in Z_{re} begins.

Given that the appearance of f_{cross} is a relatively robust phenomenon for photoresponsive films, it is important to note some practical considerations. Although f_{cross} is very consistent for a given ZnO film (typically within 10%), experimentally derived values of f_{cross} for prepared under similar conditions can vary from 500 Hz - 10 kHz. Preliminary experiments using other methods of producing ZnO (such as molten salt or solvothermal syntheses[14]) also yields f_{cross} values within this range, but the situation can be more complicated if the impedance response is not accurately described by a single parallel RC circuit. These variances from film to film are not surprising given that resistance is affected by variations in film thickness, as well as environmental factors such as humidity. Furthermore, ZnO resistivity can vary from 10^{-4} to 10^{8} Ω·cm, even in nominally undoped films, due to changes in native defects.[15] For these reasons, the optimal AC operating frequency for each photoresponsive film would need to be calibrated based on its own measured f_{cross} value.

Conclusions

We report an interesting effect in the frequency-dependent photoresponses of ZnO films: the sign reverses between low and high excitation frequencies. Our impedance data and modeling indicates that this frequency-dependent UV response can be caused by a resistance change that is induced by UV exposure, as long as there is no appreciable increase in film capacitance. Furthermore, impedance spectroscopy can be used to identify the threshold between low and high frequencies (f_{cross}) at which the change in the sign of the UV response occurs. Our findings suggest that it could be desirable to manipulate the R and C values of photodetector materials to either control – or eliminate – these frequency-dependent UV responses, which would be particularly relevant for capacitance-based sensors.

Acknowledgment

Tanzir Ahmed and Erica Hayward assisted in validating sample preparation and measurement protocols. KMP acknowledges NSERC (Canada) Discovery Grant program for funding.

ORCID

Kristin M. Poduska https://orcid.org/0000-0003-4495-0668

References

1. S.-J. Young, C.-C. Yang, and L.-T. Lai, *J. Electrochem. Soc.*, **164**, B3013 (2017).
2. L. Sang, M. Liao, and M. Sumiya, *Sensors*, **13**, 10482 (2013).
3. A. Tereshchenko, M. Bechelany, R. Viter, V. Khranovskyy, V. Smyntyna, N. Starodub, and R. Yakimova, *Sens. Actuators B: Chemical*, **229**, 664 (2016).
4. M. R. Alenezi, A. S. Alshammari, K. D. G. I. Jayawardena, M. J. Beliatis, S. J. Henley, and S. R. P. Silva, *J. Phys. Chem. C*, **117**, 17850 (2013).
5. A. J. Morfa, B. I. MacDonald, J. Subbiah, and J. J. Jasieniak, *Sol. Energ. Mat. Sol. Cells*, **124**, 211 (2014).
6. E. Espid and F. Taghipour, *ECS J. Solid State Sci. Technol.*, **7**, Q3089 (2018).
7. J.-C. Lin, B.-R. Huang, and T.-C. Lin, *J. Electrochem. Soc.*, **160**, H509 (2013).
8. R. Martins, R. Igreja, I. Ferreira, A. Marques, A. Pimentel, A. Goncalves, and E. Fortunato, *Mater. Sci. Eng. B*, **118**, 135 (2005).
9. J. Cheng and K. M. Poduska, *Nanomater.*, **3**, 317 (2013).
10. J. Cheng, M. A. Rasheed, and K. M. Poduska, *ECS J. Solid State Sci. Technol.*, **2**, Q23 (2013).
11. L. B. Rockland, *Anal. Chem.*, **32**, 1375 (1960).
12. A. S. Bondarenko and G. A. Ragoisha, In *Progress in Chemometrics Research*; A. L. Pomerantsev, Ed.; Nova Science Publishers, 2005; Chapter software is available online at http://www.abc.chemistry.bsu.by/vi/analyser/, pp 89.
13. C. Soci, A. Zhang, B. Xiang, S. A. Dayeh, D. P. R. Aplin, J. Park, X. Y. Bao, Y. H. Lo, and D. Wang, *Nano Lett.*, **7**, 1003 (2007).
14. J. Cheng and K. M. Poduska, *ECS J. Solid State Sci. Technol.*, **3**, P133 (2014).
15. J. L. Lyons, J. B. Varley, D. Steiauf, A. Janotti, and C. G. Van de Walle, *J. Appl. Phys.*, **122**, 035704 (2017).